Parametric Data Analysis of Bistable Stochastic Systems

T.D. Frank[1*], M. Sondermann[2], T. Ackemann[2,3], and R. Friedrich[1]

[1] *Institute for Theoretical Physics, University of Münster, Wilhelm-Klemm-Str. 9, 48149 Münster, GERMANY*
[2] *Institute of Applied Physics, University of Münster, Corrensstraße 2/4, 48149 Münster, GERMANY*
[3] *Department of Physics, University of Strathclyde, 107 Rottenrow, Glasgow G4 ONG, Scotland, UNITED KINGDOM*
[*] E-mail: tdfrank@uni-muenster.de

(Received 26 January 2005)

A data analysis method is proposed to derive drift and diffusion functions of Markov diffusion processes in terms of function series and expansion coefficients. The data analysis method is exemplified for a generic bistable stochastic systems involving a double-well potential and for a vertical-cavity surface-emitting laser system exhibiting an optical bistability.

Key words: data analysis, Markov processes, bistability, optical bistability

PACS numbers: 05.40.-a; 05.45.Tp; 42.65.Pc

1 Introduction

Bistability is a characteristic feature of many systems in the animate and inanimate nature. In particular, in nonequilibrium systems bistability often emerges due to symmetry breaking nonequilibrium phase transitions [1]. Examples range from biochemical systems exhibiting multistable spatiotemporal patterns [2] to bi- and multistable ecological systems [3] and bistable neural systems, perceptual systems, and motor control systems [4, 5, 6]. Bistability also plays a crucial role in many optical systems [7], a rather recent and technologically relevant example being vertical-cavity surface-emitting lasers (VCSELs, e.g. [8, 9]), which are used in data communications and sensing applications.

A fundamental model for stochastically driven bistable systems is a Brownian walk in a bistable potential [10, 11]. In the present study, we show how to derive the potential parameters from experimental data. To this end, in Sections 2.1 and 2.2 we will first review a data analysis technique that has been developed to estimate the drift and diffusion coefficients of Markov diffusion processes [12, 13]. In Sect. 2.3 we will modify this data analysis technique in order to carry out a parametric approach that is tailored to address bistable systems. The power of the modified data analysis technique will be demonstrated by studying a random walk in a double well potential (Sect. 2.4) and by extracting potential parameters of VCSELs (Sect. 2.5).

VCSELs usually show two orthogonally polarized modes with linear polarization that compete with each other (e.g. [8, 9]). In many cases, there is an noticeable interval of injection current in which both polarization modes are (locally) stable; that is, there is polarization bistability [9, 14, 15, 16, 17]. Due to fluctuating forces, the intensity of the laser light permanently switches from the one mode to the other [14, 15, 16, 17]. Many aspects of the microscopic mechanisms of polarization competition are still a matter of debate (e.g. [9, 18, 19, 20, 21]). Hence, it appears to be useful to estimate at least the parameters, for example of the bistable potential, on a macroscopic level using the experimentally obtained time series. Our approach generalizes previous works (e.g. [14, 16, 17], see Sect. 3 for a more detailed discussion).

2 Parametric data analysis of bistable stochastic systems

2.1 Basics

We consider a one-dimensional bistable stochastic system with state variable $X(t)$ that satisfies the stochastic differential equation

$$\frac{\mathrm{d}}{\mathrm{d}t}X(t) = h(X) + F(X,t) \ . \tag{1}$$

Here, h is a potential force related to

$$h(x) = -\frac{\mathrm{d}}{\mathrm{d}x}V(x) \ , \tag{2}$$

where V denotes a bistable potential with minima at $x = A$ and $x = B$. $F(x,t)$ denotes a fluctuating force that might dependent on the state variable. We assume that due to the stochastic driving force $F(x,t)$ the system performs a random walk between the minima A and B. Furthermore, we assume that the system can be approximately regarded as a Markovian system that exhibits a Markov diffusion process such that Eq. (1) can be written as

$$\frac{\mathrm{d}}{\mathrm{d}t}X(t) = h(X) + \sqrt{2D(X)}\Gamma(t) \ , \tag{3}$$

where h and D now correspond to the drift and diffusion coefficients (1st and 2nd Kramers-Moyal coefficients) of the Markov diffusion process [11]. $\Gamma(t)$ is a Langevin force with $\langle\Gamma\rangle = 0$ and $\langle\Gamma(t)\Gamma(t')\rangle = \delta(t-t')$. Accordingly, the probability density $P(x,t) = \delta(x - X(t))$ satisfies the Fokker-Planck equation [11]

$$\frac{\partial}{\partial t}P = -\frac{\partial}{\partial x}hP + \frac{\partial^2}{\partial x^2}DP \ . \tag{4}$$

By definition, the drift and diffusion coefficients can be expressed in terms of conditional averages $M_1(t')|_{X(t)=x} = \langle X(t')\rangle|_{X(t)=x}$ and $\sigma^2(t')|_{X(t)=x} = \langle X^2(t')\rangle - \langle X(t')\rangle^2\Big|_{X(t)=x}$ involving the first moment $M_1(t')$ and the variance $\sigma^2(t')$. We have

$$\left.\frac{\mathrm{d}}{\mathrm{d}t'}M_1(t')\right|_{X(t)=x,t'=t} = h(x) \ , \tag{5}$$

$$\left.\frac{1}{2}\frac{\mathrm{d}}{\mathrm{d}t'}\sigma^2(t')\right|_{X(t)=x,t'=t} = D(x) \ . \tag{6}$$

Note that the conditional averages $M_1(t')|_{X(t)=x}$ and $\sigma^2(t')|_{X(t)=x}$ are not necessarily continuously differentiable functions with respect to t'. Therefore, it is important to note that the derivatives correspond to derivatives from above. That is, we have $\mathrm{d}A(t')/\mathrm{d}t' = [A(t'+\Delta t) - A(t')]/\Delta t$ with $\Delta t \downarrow 0$, where A may correspond to M_1 or σ^2. In particular, we get

$$\begin{aligned}&\left.\frac{\mathrm{d}}{\mathrm{d}t'}\sigma^2(t')\right|_{X(t)=x,t'=t}\\ &= \left.\left\langle\frac{\mathrm{d}}{\mathrm{d}t}X^2(t)\right\rangle\right|_{X(t)=x} - 2x\left.\left\langle\frac{\mathrm{d}}{\mathrm{d}t}X(t)\right\rangle\right|_{X(t)=x}\\ &= \lim_{\Delta t\downarrow 0}\frac{1}{\Delta t}\left.\left\langle[X(t+\Delta t) - X(t)]^2\right\rangle\right|_{X(t)=x} \ .\end{aligned} \tag{7}$$

Let Ω denote the phase space of x. In the context of data analysis techniques, it is helpful to discretize Ω into bins. That is, we introduce disjoint intervals $I_i = [x_i, x_i + \Delta x)$ with $x_i = i\Delta x + x_0$ and $i = 0,\ldots,N$. While Eqs. (5) and (6) hold for every point x of the phase space Ω, similar relations can be found for the bins I_i of Ω. More precisely, from Eqs. (5) and (6) it follows that

$$\left.\frac{\mathrm{d}}{\mathrm{d}t'}M_1(t')\right|_{X(t)\in I_i,t'=t} = \langle h(X)\rangle|_{X(t)\in I_i} \ , \tag{8}$$

$$\left.\frac{1}{2}\frac{\mathrm{d}}{\mathrm{d}t'}\sigma^2(t')\right|_{X(t)\in I_i,t'=t} = \langle D(X)\rangle|_{X(t)\in I_i} \ . \tag{9}$$

2.2 Step-wise decomposition of h and D

The decomposition of the phase space Ω into bins suggests to decompose h and D in a similar way. To this end, we introduce the indicator function

$$\chi_n(x) = \begin{cases} 1 & : \ x \in I_n \\ 0 & : \ \text{otherwise} \end{cases} \ . \tag{10}$$

Then, h and D can be expressed as

$$h(x) = \sum_{n=0}^{M} a_n\chi_n(x) + O(\Delta x) \ , \tag{11}$$

$$D(x) = \sum_{n=0}^{M} b_n\chi_n(x) + O(\Delta x) \tag{12}$$

for $M = N$, where $O(\Delta x)$ correspond to terms of order Δx. This representation implies that

$$a_i = \langle h(X) \rangle|_{X(t)\in I_i} + O(\Delta x) \;, \quad (13)$$
$$b_i = \langle D(X) \rangle|_{X(t)\in I_i} + O(\Delta x) \;. \quad (14)$$

From Eqs. (8), (9), (13), and (14) it is clear that the coefficients a_i and b_i can be determined by means of

$$a_i = \frac{\mathrm{d}}{\mathrm{d}t'} M_1(t') \Big|_{X(t)\in I_i, t'=t} + O(\Delta x) \;, \quad (15)$$
$$b_i = \frac{1}{2} \frac{\mathrm{d}}{\mathrm{d}t'} \sigma^2(t') \Big|_{X(t)\in I_i, t'=t} + O(\Delta x) \;. (16)$$

In order to apply these relations to experimental data recorded with at sampling frequency $f = 1/\Delta t$, the time-derivatives are given by $\mathrm{d}A(t')/\mathrm{d}t' = [A(t'+\Delta t) - A(t')]/\Delta t + O(\Delta t)$ for $A = M_1$ and $A = \sigma^2$, respectively, where $O(\Delta t)$ describes terms of order Δt. In sum, we get

$$a_i = \frac{1}{\Delta t} \langle X(t+\Delta t) - X(t) \rangle|_{X(t)\in I_i} + O(\Delta x, \Delta t) \;, \quad (17)$$
$$b_i = \frac{1}{2\Delta t} \left\langle [X(t+\Delta t) - X(t)]^2 \right\rangle \Big|_{X(t)\in I_i} + O(\Delta x, \Delta t) \;. \quad (18)$$

The step-wise decomposition of h and D has been successfully applied in various cases [12, 13, 22, 23, 24, 25, 26]. However, the step-wise decomposition does not account for a priori information that might be available. For example, if it is reasonable to assume that the drift function h is basically given by a few first terms of a Taylor expansion (or a Fourier series), it would be of interest to determine the expansion coefficients (or Fourier coefficients) instead of the coefficients a_i and b_i. This issue of a function series expansion of h and D is addressed next.

2.3 Function series expansions of h and D

We assume now that the drift and diffusion functions can be expressed in terms of truncated function series expansions like

$$h(x) = \sum_{n=0}^{M} a_n \phi_n(x) + h_r(x) \;, \quad (19)$$
$$D(x) = \sum_{n=0}^{\tilde{M}} b_n \tilde{\phi}_n(x) + D_r(x) \;, \quad (20)$$

where h_r and D_r are remainder terms that account for the fact that we use finite expansion series. For the sake of convenience, let us L_i and $\tilde{L}_i$ denote the conditional averages

$$L_i = \frac{1}{\Delta t} \langle X(t+\Delta t) - X(t) \rangle|_{X(t)\in I_i} \;, \quad (21)$$
$$\tilde{L}_i = \frac{1}{2\Delta t} \left\langle [X(t+\Delta t) - X(t)]^2 \right\rangle \Big|_{X(t)\in I_i} \quad (22)$$

such that

$$\frac{\mathrm{d}}{\mathrm{d}t'} M_1(t') \Big|_{X(t)\in I_i, t'=t} = L_i + O(\Delta t) \;, (23)$$
$$\frac{1}{2} \frac{\mathrm{d}}{\mathrm{d}t'} \sigma^2(t') \Big|_{X(t)\in I_i . t`=t} = \tilde{L}_i + O(\Delta t) \;. (24)$$

Next, define the matrices

$$R_{in} = \langle \phi_n(X) \rangle|_{X(t)\in I_i} \;, \quad (25)$$
$$\tilde{R}_{in} = \left\langle \tilde{\phi}_n(X) \right\rangle \Big|_{X(t)\in I_i} \;. \quad (26)$$

Substituting Eqs. (19,...,26) into Eqs. (8) and (9) and exploiting the fact that the conditional averages $\langle h_r \rangle|_{I_i}$ and $\langle D_r \rangle|_{I_i}$ of the remainder terms h_r and D_r are only of the order Δx, it follows that the algebraic relations

$$L_i = \sum_{n=0}^{M} R_{in}\, a_n + O(\Delta x, \Delta t) \;, \quad (27)$$
$$\tilde{L}_i = \sum_{n=0}^{\tilde{M}} \tilde{R}_{in}\, b_n + O(\Delta x, \Delta t) \quad (28)$$

hold. The total correction terms $O(\Delta x, \Delta t)$ are now of order Δx and Δt. Note that they arise from the fact that we treat all data points equal that fall into an discretization interval of width Δx and a sample interval of length Δt. This corrections terms can be regarded as random errors that are different for different intervals. Consequently, Eqs. (27) and (28) can be interpreted as linear regression models of the form

$$L_i = \sum_{n=0}^{M} R_{in}\, a_n + e_i \ , \quad (29)$$

$$\tilde{L}_i = \sum_{n=0}^{\tilde{M}} \tilde{R}_{in}\, b_n + \tilde{e}_i \ , \quad (30)$$

where e_i and $\tilde{e}_i$ correspond to the aforementioned errors. For $M, \tilde{M} < N$ the parameters a_n and b_n can be estimated by requiring that the mean square quadratic errors

$$E = \sum_i \left| L_i - \sum_{n=0}^{M} R_{in}\, a_n \right|^2 \ , \quad (31)$$

$$\tilde{E} = \sum_i \left| \tilde{L}_i - \sum_{n=0}^{M} R_{in}\, b_n \right|^2 \quad (32)$$

become minimal. The goodness of the fit such obtained can be quantified by computing the variances σ_e^2 and $\tilde{\sigma}_e^2$ of the errors e_i and $\tilde{e}_i$ or by calculating the respective R^2-values (goodness of fit coefficients) [27].

2.4 Example: symmetric double-well potential

In order to illustrate the aforementioned procedure, we study a random walk defined by

$$\frac{\mathrm{d}}{\mathrm{d}t} X(t) = h(X) + \sqrt{2Q}\,\Gamma(t) \quad (33)$$

that involves a symmetric bistable potential given by

$$h(x) = ax + bx^3 \ , \quad (34)$$

$$V(x) = -\frac{a}{2}x^2 - \frac{b}{4}x^4 \ , \ a > 0 \ , \ b < 0 \quad (35)$$

where $Q > 0$ is the amplitude of the fluctuating force $F = \sqrt{2Q}\Gamma$. Solving Eq. (33) numerically [11], we obtained a stationary time series $X(t)$. In order to reconstructed h and V from $X(t)$ we used the four-parametric function series expansion

$$h(x) = a_0 + a_1 x + a_2 x^2 + a_3 x^3 \ . \quad (36)$$

The parameters a_i were computed from Eq. (29) and time averaging. Fig. 1 shows the drift function h as used in the simulation (dashed line) and h as obtained from the reconstruction procedure (solid line). Likewise, Fig. 2 shows the potential V as used in the simulation (dashed line) and V given by $V = a_0x + a_1x^2/2 + a_2x^3/3 + a_3x^4/4$ (solid line) with a_i determine by the data analysis technique. The quality of the fit can be determined in terms of the variance σ_e^2 of the error e_i occurring in Eq. (29) and in terms of the goodness of fit parameter R^2. For our synthetically produced data set we found $\sigma_e^2 = 0.06$ and $R^2 = 0.99$. That is, 99% of the variance of the data set is explained by the four parametric regression model (36).

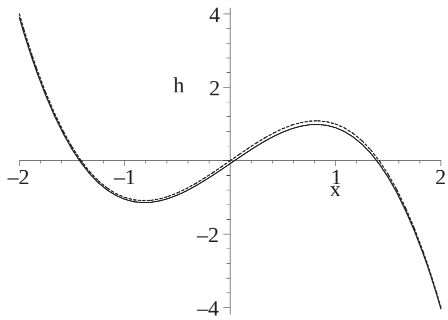

FIG. 1. Original (dashed line) and reconstructed (solid line) drift function $h(x)$ of the random walk model given by Eqs. (33) and (34). Input-parameters: $a = 2.00$, $b = -1.00$, $Q = 1.00$, $\Delta t = 0.01$, number of data points 400000. Output-parameters: $a_0 = -0.08$, $a_1 = 1.96$, $a_2 = 0.00$, $a_3 = -0.99$.

2.5 Optical bistability of VCSELs

As mentioned in the introduction, under particular circumstances VCSELs can exhibit an optical bistability in which two polarization modes are stable. In this case the system may permanently switch between the two modes. Consequently, the intensity of a single polarization mode jumps in a stochastic fashion back and forth between a minimum and a maximum value. We illustrate here the data analysis method presented in Sect. 2.3 by means of two time series shown in Figs. 3 and

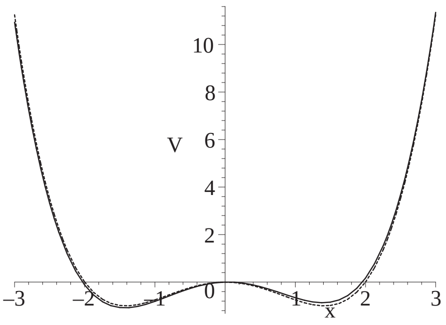

FIG. 2. Original (dashed line) and reconstructed (solid line) potential $V(x)$. Parameters as in Fig. 1.

4. The time series were recorded in an experimental setup similar to the one described in [21]. For further details, see [28]. Figs. 3 and 4 depict the intensity of one polarization mode for two different trials.

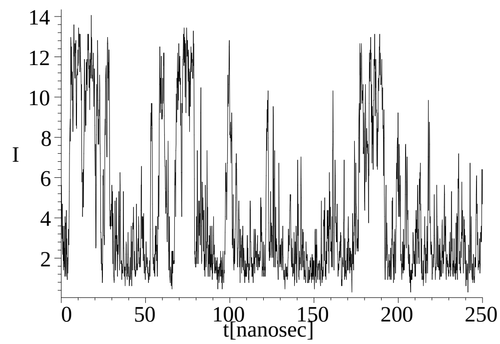

FIG. 3. Time series of a random walk given by the intensity of a VCSEL-polarization mode. Only a detail is shown. Total recording time was 50000 ns; sampling interval $\Delta t = 0.125$ ns; number of data points 400000. Intensity is shown in arbitrary units.

Assuming that the drift force is given by the four-parametric function

$$h(I) = a_0 + a_1 I + a_2 I^2 + a_3 I^3 \qquad (37)$$

related to the potential

$$V(I) = a_0 I + \frac{a_1}{2} I^2 + \frac{a_2}{3} I^3 + \frac{a_3}{4} I^4 \ , \qquad (38)$$

we have estimated the parameters a_i from the trajectories $I(t)$ by means of Eqs. (23,...,32) and

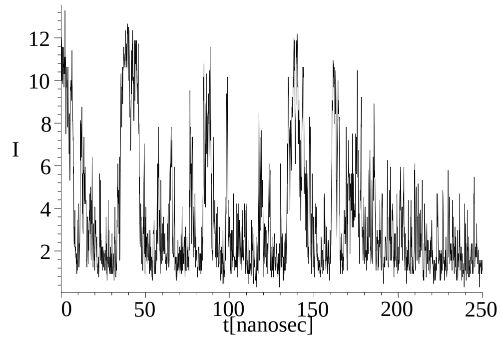

FIG. 4. Intensity of a VCSEL-polarization mode as in Fig. 3 for another trial recorded for slightly different system parameters.

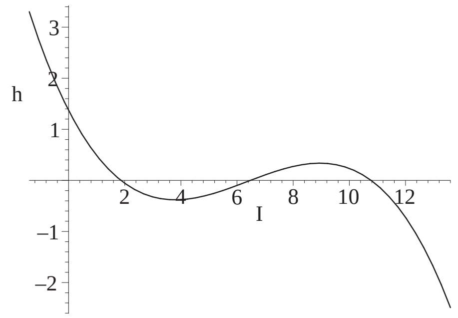

FIG. 5. Drift function $h(I, a_0, \ldots, a_3)$ of the intensity hopping shown in Fig. 3 as obtained from the parametric data analysis technique discussed in Sect. 2.3.

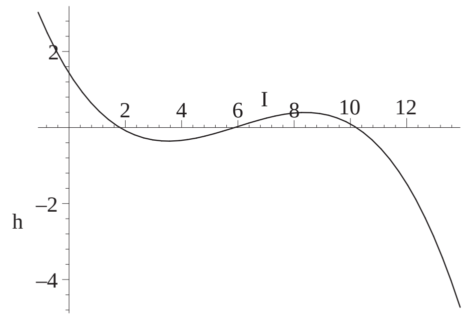

FIG. 6. Drift function $h(I, a_0, \ldots, a_3)$ of the intensity hopping shown in Fig. 4.

time averaging. The result is shown in Figs. 5 and 6 in terms of the drift functions $h(I; a_0, \ldots, a_3)$

and in Figs. 7 and 8 in terms of the corresponding potentials $V(I; a_0, \ldots, a_3)$. In the drift functions the two preferred intensity values are reflected as intersection points with the x-axes with negative slopes. In the potentials the preferred intensity values correspond to the potential minima. The optical bistability is related to the bistability of the potentials. The linear regression models underlying Figs. 5 and 6 exhibit variances of $\sigma_e^2 = 0.06$ and $\sigma_e^2 = 0.06$, respectively. The R^2-values are $R^2 = 0.89$ and $R^2 = 0.90$. That is, the models explain about 90% of the variance of the respective data sets.

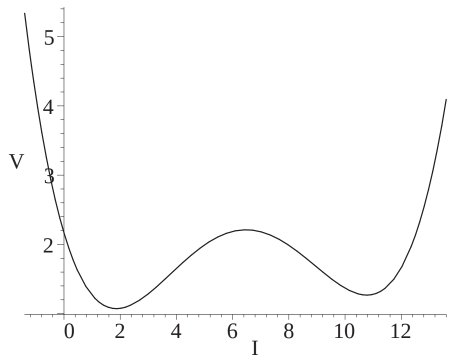

FIG. 7. Potential $V(I, a_0, \ldots, a_3)$ of the intensity hopping shown in Fig. 3 as obtained from the parametric data analysis technique discussed in Sect. 2.3.

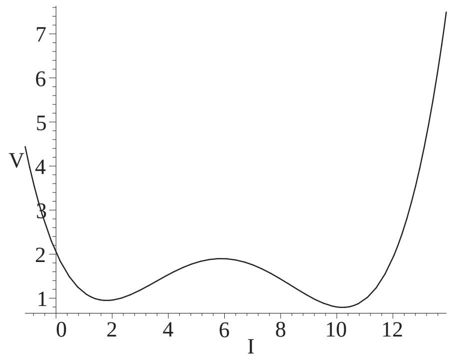

FIG. 8. Potential $V(I, a_0, \ldots, a_3)$ of the intensity hopping shown in Fig. 4.

3 Conclusions

We have proposed a new data analysis technique that yields estimates for drift and diffusion functions of Markov diffusion processes. Accordingly, drift and diffusion functions are given in terms of truncated function series with expansion parameters computed from experimental data. In particular, we have shown that our approach reduces to a previously introduced data analysis technique [12, 13] if drift and diffusion functions are expressed in terms of a sum of indicator functions (compare Sections 2.2 and 2.3). As exemplified by a generic model for a bistable stochastic process (double-well potential model), the proposed data analysis works well for moderately large data sets. In addition, we applied our data analysis approach to derive potential functions for bistable VCSELs. The potentials thus obtained were double-well potentials. That is, the optical bistability was reflected by potentials that exhibit two minima. In this context, potential functions have already been derived from experimental data in previous studies [14, 16, 17]. In these studies, however, the potentials were reconstructed on the basis of probability density functions of intensity signals assuming that the diffusion coefficient is a state-independent function. Consequently, these reconstruction methods actual yielded estimates for pseudo potentials that are (roughly speaking) given by ratios of potential functions and diffusion constants. In contrast, our approach derives potential functions from experimental data in a direct fashion and, consequently, represents a direct access to potential functions. Finally, we would like to mention that alternatively to the Brownian dynamics approach, polarization switching of VCSELs may also be described in terms of master equations [29]. In this context, it is important to realize that master equation approaches and Brownian dynamics approaches are closely related to each other because under certain circumstances master equations can be approximately expressed in terms of Brownian walk models such as given by Eq. (1).

References

[1] H. Haken. *Synergetics: Itroduction and Advanced topics.* (Springer, Berlin, 2004).

[2] M. C. Cross and P. C. Hohenberg. Rev. Mod. Phys. **65**, 851 (1993).

[3] R. M. May. Nature. **261**, 459 (1976).

[4] H. Haken. *Synergetic computers and cognition.* (Springer, Berlin, 1991).

[5] J. A. S. Kelso. *Dynamic patterns - The self-organization of brain and behavior.* (MIT Press, Cambridge, 1995).

[6] T. D. Frank, A. Daffertshofer, C. E. Peper, P. J. Beek, and H. Haken. Physica D. **144**, 62 (2000).

[7] H. M. Gibbs. *Optical Bistability: Controlling Light with Light.* (Academic Press, Orlando, 1985).

[8] C. J. Chang-Hasnain, J. P. Harbison, G. Hasnain, A. von Lehmen, L. T. Florez, and N. G. Stoffel. Electron. Lett. **27**, 163 (1991).

[9] K. D. Choquette, R. P. Schneider Jr., K. L. Lear, and R. E. Leibenguth. IEEE J. Selec. Top. Quantum Electron. **1**, 661 (1995).

[10] P. Hänggi and H. Thomas. Phys. Rep. **88**, 207 (1982).

[11] H. Risken. *The Fokker-Planck equation — Methods of solution and applications.* (Springer, Berlin, 1989).

[12] R. Friedrich and J. Peinke. Phys. Rev. Lett. **78**, 863 (1997).

[13] S. Siegert, R. Friedrich, and J. Peinke. Phys. Lett. A **243**, 275 (1998).

[14] G. Giacomelli, F. Marin, M. Gabrysch, K. H. Gulden, and M. Moser. Opt. Commun. **146**, 136 (1998).

[15] M. B. Willemsen, M. U. F. Khalid, M. P. van Exter, and J. P. Woerdman. Phys. Rev. Lett. **82**, 4815 (1999).

[16] S. Barbay, G. Giacomelli, and F. Marin. Phys. Rev. E **61**, 157 (2000).

[17] B. Nagler, M. Peeters, J. Albert, G. Verschaffelt, K. Panajotov, H. Thiehpont, I. Veretnnicoff, J. Danckaert, S. Barbay, G. Giacomelli, and F. Marin. Phys. Rev. A **68**, 013813 (2003).

[18] J. Martín-Regalado, F. Prati, M. S. Miguel, and N. B. Abraham. IEEE J. Quantum Electron. **33**, 765 (1997).

[19] J. Danckaert, B. Nagler, J. Albert, K. Panajotov, I. Veretennicoff, and T. Erneux. Opt. Commun. **201**, 129 (2002).

[20] B. S. Ryvkin, E. A. Avrutin, and M. Pessa. J. Appl. Phys. **93**, 2353 (2003).

[21] M. Sondermann, M. Weinkath, and T. Ackeman. IEEE J. Quantum Electron. **40**, 97 (2004).

[22] R. Friedrich, J. Peinke, and C. Renner. Phys. Rev. Lett. **84**, 5224 (2000).

[23] J. Gradisek, S. Siegert, R. Friedrich, and I. Grabec. Phys. Rev. E **62**, 3146 (2000).

[24] G. R. Jafari, S. M. Fazeli, F. Ghasemi, S. M. V. Allaei, M. R. R. Tabar, A. I. Zad, and G. Kavei. Phys. Rev. Lett. **91**, 226101 (2002).

[25] H. U. Bödeker, M. C. Röttger, A. Liehr, T. D. Frank, R. Friedrich, and H. G. Purwins. Phys. Rev. E **67**, 056220 (2003).

[26] J. Peinke, F. Böttcher, and S. Barth. Annalen der Physik **2004**, 450 (2004).

[27] R. E. Walpole and R. H. Myers. *Probability and Statistics for Engineers and Scientists.* (MacMillian Publishers, New York, 1985).

[28] M. Sondermann, *Doctoral Thesis: On polarization dynamics in vertical cavity surface emitting lasers* (Münster, 2004), http://miami.uni-muenster.de/.

[29] J. A. Freund, S. Barbay, S. Lepri, and G. Giacomelli. Fluctuation and Noise Letters **3**, L195 (2003).